Eur. J. Stat. 6 (2026) 10
doi: 10.28924/ada/stat.6.10

Autocorrelation Structure of a Novel Generalized Harmonically Weighted Process

Djillali Seba[1,2]

[1] *Ecole Supérieure en Informatique, Sidi Bel Abbes, Algeria*
[2] *Applied Mathematics Laboratory, University of Bejaia, Bejaia, Algeria*
d.seba@esi-sba.dz

Abstract. The main objective of our work is to introduce a new generalization of Harmonically Weighted process to enhance the model's flexibility by incorporating the parameter a, we establish several properties of the proposed model, including the harmonic inverse transformation, spectral density and autocorrelation function. The model demonstrates a capacity to capture short, long, and moderately long memory. Its persistence and memory characteristics are analyzed theoretically using the spectral density, autocorrelation function, and impulse response function. Furthermore, we compare the Moderate Harmonically Weighted (M-HW) process with related models such as Harmonically Weighted process, ARFIMA, and GAR models. We conduct a simulation study to check the validity of the theoretical findings, providing graphically the spectrum, ACF and IRF for our model, followed by comparisons with its competitors.

1. Introduction

Time series analysis has gained a widespread attention among researchers over last decades, especially in applied fields such as finance ([28], [8], [1], [9]), hydrology ([23], [20], [25]), epidemiology ([19], [27] , [30]), and climatology ([11], [12], [24]).

In the early 1970s, the Box-Jenkins [7] method was introduced, based on the three core components: autoregression, differencing, and moving average. In this framework, the differencing degree is an integer.

Later, in 1980, Granger and Joyeux [13], and Hosking [17] in 1981 defined a new model "fractional ARIMA" by allowing the differencing parameter to be fractional.

This model is notable for its ability to handle long memory, where the effect of a shock vanishes slowly. Mathematically, the sum of the auto-correlations is infinite Baillie [3]. Moreover, fractional differencing is crucial in solving the problem of cause over-differencing, which will lead to the loss of information Huang [18].

Several extensions of ARFIMA process have been proposed. Gray et al. [14] introduced ARFIMA with quasi-periodic behavior, Peiris et al. [22] presented a flexible model GAR(1) to model long

Received: 4 Oct 2025.
Key words and phrases. IRF; Harmonically Weighted process; Persistence; Spectrum; GAR; long memory.

memory and weak-long memory, Sabzikar et al. [26] introduced Tempered ARFIMA (ARTFIMA), while Bhootana et al. [5] generalized GARMA model basing on Humbert polynomial. Several studies have explored time-varying ARFIMA models, which are capable of capturing regime changes in long-memory time series, such as those presented in [29] and [6]. [2] Amimour et al. defined a periodic degree of fractional parameter, Benaklef et al. [4] incorporated a periodic coefficient into the fractionally integrated model.

An alternative way to define a long memory model was suggested by Hassler [16], known as Harmonically Weighted Process (HW). This model does not require the estimation of the parameter d, but it may still capture long memory, though less effectively than a fractional autoregressive process. The HW process has an unbounded spectrum at the origin and the sum of autocorrelations is infinite but its square sum is finite, see([10]).

A further extension of HW process has been presented in [21] who considered cyclic long memory, know as Generalized Harmonically Weighted (GHW) process, and it is defined as follows

$$\begin{aligned} y_t &= \mu + \sum_{j=0}^{\infty} \frac{1 - 2\eta L + L^2}{2L} \\ &= \mu + \sum_{j=0}^{\infty} \frac{\cos(\lambda_g(j+1))}{j+1} x_{t-j}, \end{aligned}$$

Where L is lag operator and $\eta = \cos(\lambda_g)$.

The main goal of this work is to extend the results in Hassler et al. [16]. To do this, by introducing a real-valued parameter a into the lag operator, thereby increasing the model's flexibility and making the memory properties dependent on a.

The remainder of the manuscript is set out as follows, the first section introduces the Moderate Harmonically Weighted (M-HW) process along with its harmonic inverse transformation. In the second section, we analyze the spectral density and autocorrelation function. The third section presents a comparison of the proposed model with competing models, including the Harmonically Weighted (HW) process, ARFIMA, and GAR models. Finally, the paper concludes with a summary and future research perspectives.

2. Presentation of the Model: Moderate Harmonically Weighted Process (M-HW)

In this section, we present a novel model that generalizes the HW process by incorporating the parameter a , the latter is called Moderate Harmonically Weighted Process (M-HW).

We begin by defining the harmonically weighted filter $h(L)$ as follows

$$h(L) = \frac{-\ln(1 - aL)}{aL} = \sum_{j=0}^{\infty} \frac{a^j}{j+1} L^j, \tag{1}$$

L is lag operator, $|a| \leq 0$ to ensure the invertibility of the process.

When $a = 1$ it reduces to the results of [16].

Then, we present M-HW process in the following form

$$X_t = \mu + h(L)\varepsilon_t, \tag{2}$$

where $\varepsilon_t \sim WN(0, \sigma^2)$.
Thus,

$$X_t = \mu + \sum_{j=0}^{\infty} \frac{a^j}{j+1}\varepsilon_{t-j} \tag{3}$$

Applying D'Alembert criterion $\lim_{j\to\infty} \frac{a^{j+1}}{j+2}\frac{j+1}{a^j} = \lim_{j\to\infty} \frac{j+1}{j+2}a = a$,

- If $|a| \leq 1$ then $h(L) < \infty$, meaning that it converges. Conversely, if $|a| > 1$, then $h(L)$ diverges.
- If When $a = 1$, $\sum_{j=0}^{h} \frac{1}{j+1} \approx \ln(h) + \gamma$, where γ is the constant of of Euler-Mascheroni.

Now, we present the harmonic inverse transformation (HIT). It is defined as follows

$$g(L) = \frac{-aL}{\ln(1-aL)} = \sum_{j=0}^{\infty} g_j L^j, g_0 = 1. \tag{4}$$

The coefficient are similar to Gregory coefficients.

$$\frac{aL}{\ln(1-aL)} = 1 + \frac{a}{2}L - \frac{a^2}{12}L^2 + \frac{a^3}{24}L^3 - \frac{19a^4}{720}L^4 + \frac{3a^5}{160}L^5... \tag{5}$$

3. Probabilistic properties of M-HW process

Spectral density of M-HW process. We present the spectral density form of M-HW process, and its asymptotic behavior.

Proposition 3.1. *For M-HW process defined in equation 3, and under the assumption of $|a| \leq 1$, the spectral density is given by the following expression*

$$f_x(\omega) = \frac{\sigma^2}{2\pi a^2}\left(\ln^2\left(\sqrt{1+a^2-2a\cos(\omega)}\right) + \arctan^2\left(\frac{-a\sin(\omega)}{1-a\cos(\omega)}\right)\right) \tag{6}$$

Proof. For $\omega > 0$ and $\mu = 0$, we have $f_x(\omega) = |h(\exp(i\omega))|^2$
$f_\varepsilon(\omega) = \sigma^2 \frac{\ln(1-a\exp(i\omega))\ln(1-a\exp(i\omega))}{a^2}$
We calculate $\ln^2(1-a\exp(i\omega))$:
We know that $\ln^2(1-a\exp(i\omega)) = \ln^2(r(\omega)\exp(i\theta(\omega))) = \ln^2(r(\omega)) + (\theta(\omega))^2$

$$r(\omega) = \sqrt{1-a\cos(\omega)+a^2\sin^2(\omega)} = \sqrt{1+a^2-2a\cos(\omega)}$$

and

$$\theta(\omega) = \arctan\frac{-a\sin(\omega)}{1-a\cos(\omega)}$$

Finally, we combine the results to get (6).
For $h \to 0$, $f_x(\omega) \sim \ln^2(1-a) f_\varepsilon(0)$ indicating the spectral singularity at the origin. This implies that the sum of the Wold coefficients diverges at a logarithmic rate.

Autocovariance Function of M-HW process. We present the autocovariance and autocorrelation of the M-HW process, along with their asymptotic behavior .

Proposition 3.2. *The autocovariance function $\gamma_x(h)$ for M-HW process can be written in the following form*

$$\gamma_x(h) = \sigma^2 \frac{a^h}{h} \sum_{j=1}^{h} \frac{a^{2j}}{j} \tag{7}$$

Proof. knowing that $\gamma_x(h) = \mathbb{E}(X_t, X_{t+h})$

$$\begin{aligned} \mathbb{E}(X_t X_{t+h}) &= \mathbb{E}\left(\sum_{j=1}^{h} \frac{a^j}{j+1} \varepsilon_{t-j} \sum_{j=0}^{h} \frac{a^{j+h}}{j+h+1} \varepsilon_{t-j+h} \right) \\ &= \sigma^2 \sum_{j=0}^{h} \frac{a^{2j+h}}{(j+1)(j+h+1)} \\ &= \sigma^2 \frac{a^h}{h} \sum_{j=1}^{h} \frac{a^{2j}}{j}. \end{aligned}$$

Using the same arguments, the variance is expressed as follows $Var(X_t) = \sigma^2 \sum_{j=1}^{\infty} \frac{a^{2j}}{j^2}$. Thus, we combine $\gamma_x(h)$ and $Var(X_t)$ to get the autocorrelation function.

$$\rho_x(h) = \frac{a^h}{h} \frac{\sum_{j=1}^{h} \frac{a^{2j}}{j}}{\sum_{j=1}^{\infty} \frac{a^{2j}}{j^2}}. \tag{8}$$

The asymptotic behavior of $\gamma_x(h)$ can be bounded by $\gamma_x(h) \leq \sigma^2 \frac{a^h}{h} \sum_{j=1}^{h} \frac{1}{j}$, since $|a^{2j}| < 1$. For the sake of simplicity, we use the approximation $\sum_{j=1}^{h} \frac{1}{j} \approx \ln(h) + \gamma$, where γ is the constant of of Euler-Mascheroni, thus $\gamma_x(h) \leq \sigma^2 \frac{a^h}{h} \ln(h)$.

Impulse response function of M-HW process. Impulse response function(IRF) is the most commonly utilized tool for calculating how shocks affect time series, this measure is based on MA(∞) representation of equation (3).
The MA coefficients in M-HW process, also known impulse response coefficients, characterize how the process reacts to shocks. The persistence of the process is defined by the rate at which these impulse responses decay to zero.

In our case the Impulse response coefficients are given by $\frac{\partial X_t}{\partial \varepsilon_{t-j}} = \frac{a^{2j}}{j+1}$ This is clearly lower than the impulse response coefficients of the HW process $\frac{1}{j+1}$ because $|a| < 1$, confirming that the latter is more persistent than the M-HW process.

4. Comparison of M-HW process with Fractional Integrated process

In this section, we compare between M-HW process and different models such as HW process and Fractional integrated process. We focus particularly on the fractional autoregressive model defined in [13], and GAR(1) introduced by [22], The comparison is based on the concepts of persistence and memory characteristics.

Harmonically weighted process is defined as follows

$$X_t = \mu + \sum_{j=0}^{\infty} \frac{1}{j+1} \varepsilon_{t-j}, \tag{9}$$

$\varepsilon_t \sim WN(0, \sigma^2)$

The moving average presentation of ARFIMA(0,d,0) expression is presented as follows

$$X_t = \sum_{j=0}^{\infty} \frac{\Gamma(j+d)}{\Gamma(d)\Gamma(j+1)} \varepsilon_{t-j} \tag{10}$$

$|d| \in \frac{1}{2}$, $\varepsilon_t \sim WN(0, \sigma^2)$.

The moving average presentation of GAR(1) is in the following form

$$X_t = \sum_{j=0}^{\infty} \frac{\Gamma(j+d)}{\Gamma(d)\Gamma(j+1)} a^j \varepsilon_{t-j} \tag{11}$$

$|a| < 1, \quad d \in \mathbb{R}$, $\varepsilon_t \sim WN(0, \sigma^2)$

According to Hassler [15] the persistence is the sum of autocovariance and the concept of memory based on the absolute sum of autocovariance.

- GAR(1) is more persistent than M-HW process if $\ln^2(1-a) < (1-a)^{-2d}$, this inequality holds when a is close to 0, indicating that the persistence of M-HW process depends on the value of a.
- ARFIMA (0,d,0) is more persistent than GAR(1). Consequently, M-HW process is less persistent if the following inequality holds $\ln^2(1-a) < (4\sin^2(\frac{\omega}{2}))^{-2d}$.
- HW process is persistent than M-HW process if $\ln^2(1-a) < \ln^2(\omega)$.
- To compare between competitor models cited above basing on the autocorrelation function. we calculate the limit when $h \to \infty$.
- We compute the following limits $\lim_{h\to\infty} \frac{ACF_{M-HW}}{ACF_{HW}} = \lim_{h\to\infty} \frac{a^h \ln(h)/h}{\ln(h)/h} = 0$ when $|a| < 1$, in the case of a=1, it reduces to the results of [16].
- $\lim_{h\to\infty} \frac{ACF_{M-HW}}{ACF_{FI}} = \lim_{h\to\infty} \frac{a^h \ln(h)/h}{h^{2d-1}} = 0$

- $\lim_{h\to\infty} \frac{ACF_{M-HW}}{ACF_{GAR}} = \lim_{h\to\infty} \frac{a^h \ln(h)/h}{a^h h^{d-1}} = 0$, for $0 < d < 1/2$
- These results justify the term "moderate", in the Moderate Harmonically Weighted (M-HW) process. Due to its decay structure, the M-HW process exhibits the lowest level of persistence among the models considered.

To discuss the process' memory, we have to treat the absolute sum of autocovariance function

$$\begin{aligned} |\gamma_x(h)| &= |\frac{a^h}{h}\sum_{j=1}^{h}\frac{a^{2j}}{j}| \\ &\leq \frac{|a^h|}{h}\sum_{j=1}^{h}\frac{|a^{2j}|}{j} \\ &\leq \frac{1}{h}\sum_{j=1}^{h}\frac{1}{j} \end{aligned}$$

Thus, the autocovariance function of M-HW process has "moderate" long memory and less than HW process.

In Figure(1), we illustrate the comparison between the spectra of the M-HW process and its fractional integrated competitor GAR(1), we take the value of $a = 0.7$ and we variate the values of memory parameter d.

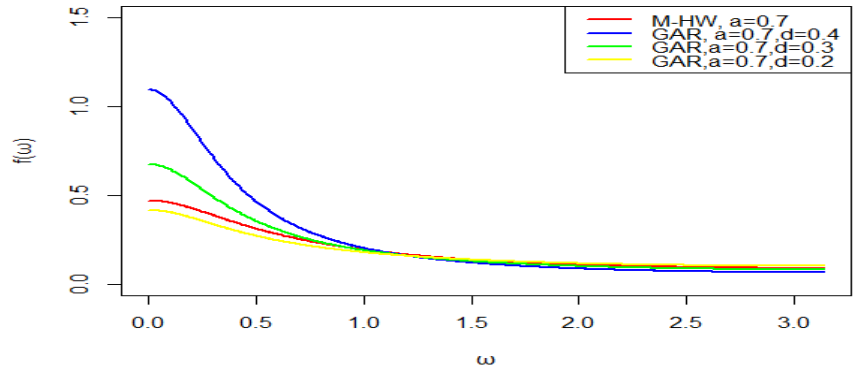

FIGURE 1. Comparison between the spectral density of M-HW process and GAR(1)

5. Simulation Study

We simulate GHW process using the truncation of its moving average representation.

$$X_t = \mu + \sum_{j=0}^{m} \frac{a^j}{j+1}\varepsilon_{t-j}, \tag{12}$$

Where $m = 1, ..., T$, $\varepsilon_t \sim N(0, \sigma^2)$. The generated model is presented in Figure (2).

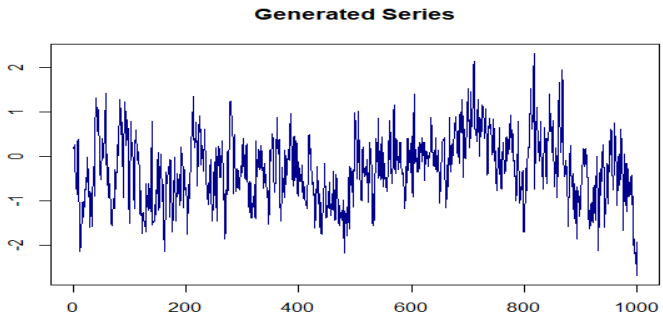

FIGURE 2. Generated Series of M-HW process for a=0.9

We present ACF of the process generated by 12 for different values of a in Figure (3) and Figure (4).

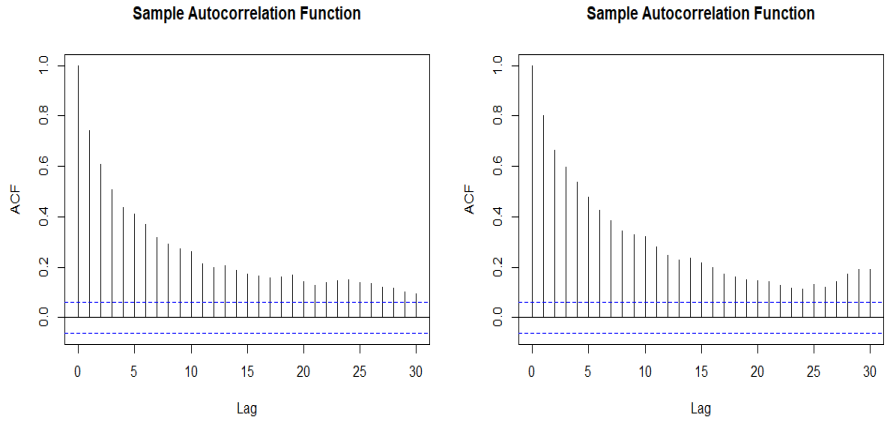

FIGURE 3. Sample Autocorrelation of M-HW, left a=0.99 ,right a=1

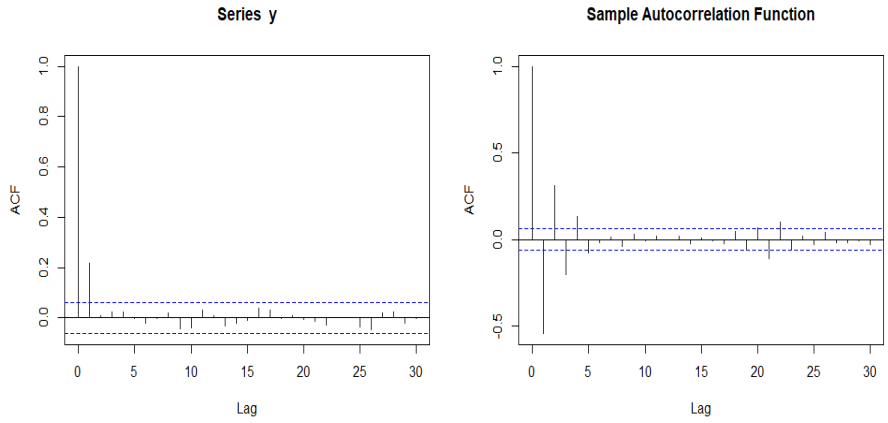

FIGURE 4. Sample Autocorrelation of M-HW, left a=0.2 ,right a=-0.8

- For a=0.9 close to 1 the M-HW process, the behavior of ACF decay slowly and quite similar to ACF of HW process which is described by a moderate long memory.
- For a=0.2 has a short memory characterized by a fast decay of ACF.
- For a negative, we get an anti-persistent process.
- Our model is more flexible due to its capacity to handle short and long memory according to the values of a.

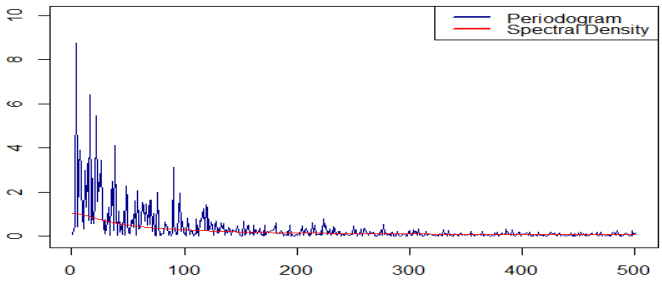

FIGURE 5. Periodogram vs Spectral density of M-HW process for a=0.9

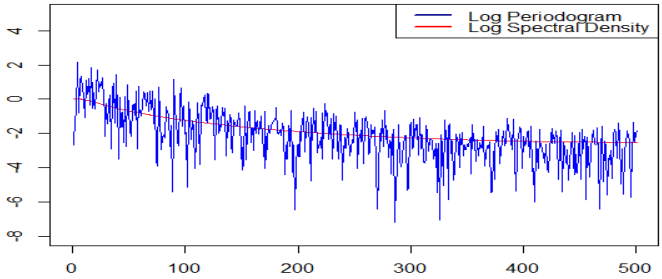

FIGURE 6. Log Periodogram vs Log Spectral density a=0.9

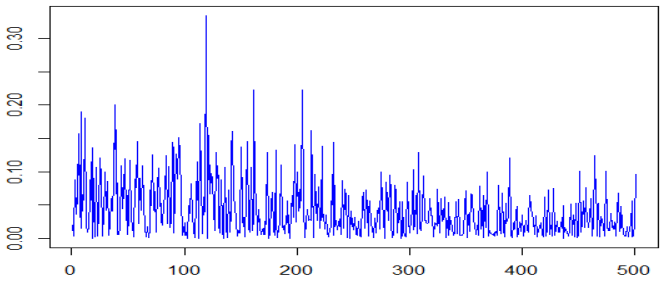

FIGURE 7. Periodogram of M-HW process for a=0.4

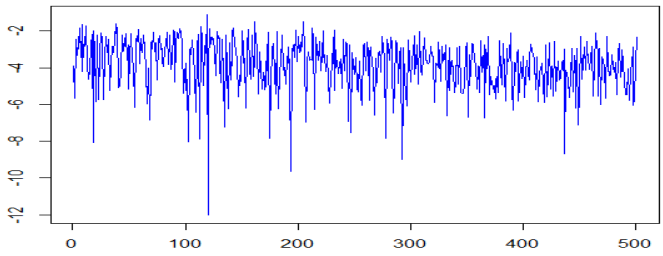

FIGURE 8. Log Periodogram of M-HW process for a=0.4

Figure (5) displays the theoretical spectrum and periodogram for $a = 0.9$, while Figure (6) presents the corresponding log-periodogram. We remark that the theoretical spectrum fits the periodogram perfectly, which exhibits an explosive behavior at the origin-an indication of long memory. In contrast, Figures (7) and (8) show the periodogram and log periodogram for $a = 0.4$, which is a value close to zero, where no such explosive behavior is observed.

To compare between the behavior of long, semi-long memory models and our models in term of persistence and memory we have presented ACF function and Impulse response function representation of M-HW, HW, ARFIMA, GAR processes for different values of a and d.

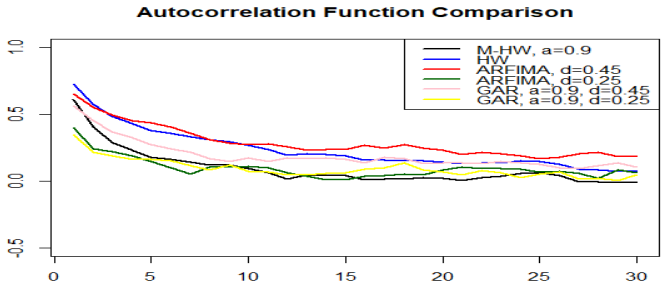

FIGURE 9. Comparison between different model M-HW, HW, ARFIMA, GAR processes for different values of a and d

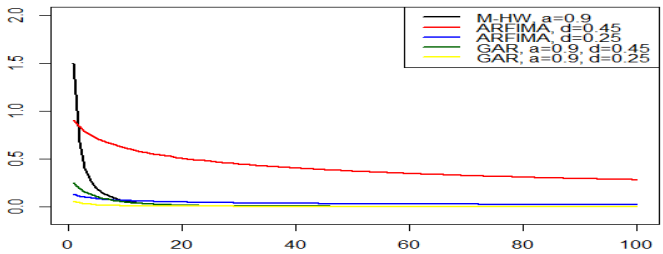

FIGURE 10. Impulse Response Function for M-HW, HW, ARFIMA, GAR processes

- We observe in Figure (9) that the autocorrelation functions of both HW and ARFIMA(0,0.45,0) decrease slowly, indicating that ARFIMA(0,0.45,0) exhibits pure long-memory behavior. In contrast, the same model with $d = 0.25$ shows a faster decay compared to all other models, including HW, ARFIMA(0,0.45,0), and M-HW.
- M-HW and GAR(1) for d=0.45, the ACF of these models are too close and has quite similar memory behavior.
- ACF of M-HW has a slowly decay comparing to ARFIMA(0,0.25,0) and GAR(1) for $d = 0.25$
- The graphical illustration of the IRF in Figure (10) confirms the validity of the theoretical findings. The M-HW process and the GAR model exhibit similar behavior, as their graphs become nearly identical starting from lag 20.
- ARFIMA is more persistent than other competitors.

Conclusion

In summary, this paper explores key time series properties to analyze the persistence and memory behavior of the proposed model. Our findings demonstrate that the model exhibits a "moderate" long-memory behavior, as confirmed theoretically through the interpretation of the ACF, IRF, and spectral function. The proposed model offers greater flexibility compared to the Harmonically Weighted process due to the inclusion of the parameter a. Specifically, for values of a close to 0, the model captures short-memory behavior, while for a close to 1, it characterizes moderate long-memory behavior.
This model can be further extended by considering a time-varying parameter a_t periodic, double-periodic, or quasi-periodic parameter. Additionally, parameter estimation can be performed using various techniques such as whittle estimator, conditional sum of squares, and generalized least squares. Future research could also explore other probabilistic properties of the model.

Acknowledgement. We acknowledge the support of "Direction Générale de la Recherche Scientifique et du Développement Technologique DGRSDT".MESRS ALGERIA.

Competing interests: The author declares that there is no conflict of interest regarding the publication of this paper.

References

[1] S. Ahmed, M.M. Alshater, A.E. Ammari, H. Hammami, Artificial Intelligence and Machine Learning in Finance: A Bibliometric Review, Res. Int. Bus. Financ. 61 (2022), 101646. https://doi.org/10.1016/j.ribaf.2022.101646.

[2] A. Amimour, K. Belaide, A Long Memory Time Series with a Periodic Degree of Fractional Differencing, arXiv:2008.01939, 2020. https://doi.org/10.48550/arXiv.2008.01939.

[3] R.T. Baillie, Long Memory Processes and Fractional Integration in Econometrics, J. Econ. 73 (1996), 5–59. https://doi.org/10.1016/0304-4076(95)01732-1.

[4] N. Benaklef, K. Belaide, Fractional Periodic Autoregression, Stochastics 97 (2025), 435–447. https://doi.org/10.1080/17442508.2025.2462816.

[5] N. Bhootna, M.S. Dhull, A. Kumar, N. Leonenko, Humbert Generalized Fractional Differenced ARMA Processes, Commun. Nonlinear Sci. Numer. Simul. 125 (2023), 107412. https://doi.org/10.1016/j.cnsns.2023.107412.

[6] L. Bisaglia, M. Grigoletto, A New Time-Varying Model for Forecasting Long-Memory Series, Stat. Methods Appl. 30 (2020), 139–155. https://doi.org/10.1007/s10260-020-00517-7.

[7] G.E.P. Box, G.M. Jenkins, G.C. Reinsel, Time Series Analysis: Forecasting and Control, Holden-Day, 1976.

[8] N. H. Chan, Time Series: Applications to Finance, Wiley, 2004.

[9] T. Cipra, Time Series in Economics and Finance, Springer, 2020. https://doi.org/10.1007/978-3-030-46347-2.

[10] M. Demetrescu, V. Kuzin, U. Hassler, Long Memory Testing in the Time Domain, Econ. Theory 24 (2008), 176–215. https://doi.org/10.1017/S0266466608080092.

[11] R. V. Donner, Nonlinear Time Series Analysis in the Geosciences: Applications in Climatology, Geodynamics and Solar-Terrestrial Physics, Springer, Berlin, 2008.

[12] C. Duchon, R. Hale, Time Series Analysis in Meteorology and Climatology: An Introduction, John Wiley & Sons, New York, 2012.

[13] C.W.J. Granger, R. Joyeux, An Introduction to Long-memory Time Series Models and Fractional Differencing, J. Time Ser. Anal. 1 (1980), 15–29. https://doi.org/10.1111/j.1467-9892.1980.tb00297.x.

[14] H.L. Gray, N. Zhang, W.A. Woodward, On Generalized Fractional Processes, J. Time Ser. Anal. 10 (1989), 233–257. https://doi.org/10.1111/j.1467-9892.1989.tb00026.x.

[15] U. Hassler, Time Series Analysis with Long Memory in View, John Wiley & Sons, New York, 2018.

[16] U. Hassler, M. Hosseinkouchack, Harmonically Weighted Processes, J. Time Ser. Anal. 41 (2019), 41–66. https://doi.org/10.1111/jtsa.12475.

[17] J.R.M. Hosking, Fractional Differencing, Biometrika 68 (1981), 165–176. https://www.jstor.org/stable/2335817

[18] S.C. Huang, Return and Volatility Contagions of Financial Markets over Difference Time Scales, Int. Res. J. Finance Econ. 42 (2010), 140–148.

[19] M.D.R.D.D.O. Latorre, M.R.A. Cardoso, Análise de Séries Temporais Em Epidemiologia: Uma Introdução Sobre Os Aspectos Metodológicos, Rev. Bras. Epidemiol. 4 (2001), 145–152. https://doi.org/10.1590/S1415-790X2001000300002.

[20] D. Machiwal, M.K. Jha, Hydrologic Time Series Analysis: Theory and Practice, Springer, 2012.

[21] F. Maddanu, A Harmonically Weighted Filter for Cyclical Long Memory Processes, AStA Adv. Stat. Anal. 106 (2021), 49–78. https://doi.org/10.1007/s10182-021-00394-9.

[22] M.S. Peiris, Improving the Quality of Forecasting Using Generalized AR Models: An Application to Statistical Quality Control, Stat. Methods 5 (2003), 156–171.

[23] J.D. Pelletier, D.L. Turcotte, Long-Range Persistence in Climatological and Hydrological Time Series: Analysis, Modeling and Application to Drought Hazard Assessment, J. Hydrol. 203 (1997), 198–208. https://doi.org/10.1016/S0022-1694(97)00102-9.

[24] V. Privalsky, Time Series Analysis in Climatology and Related Sciences, Springer, 2021. https://doi.org/10.1007/978-3-030-58055-1.

[25] B. Ramadevi, K. Bingi, Chaotic Time Series Forecasting Approaches Using Machine Learning Techniques: A Review, Symmetry 14 (2022), 955. https://doi.org/10.3390/sym14050955.

[26] F. Sabzikar, M.M. Meerschaert, J. Chen, Tempered Fractional Calculus, J. Comput. Phys. 293 (2015), 14–28. https://doi.org/10.1016/j.jcp.2014.04.024.

[27] L. Tomov, L. Chervenkov, D.G. Miteva, H. Batselova, T. Velikova, Applications of Time Series Analysis in Epidemiology: Literature Review and Our Experience during COVID-19 Pandemic, World J. Clin. Cases 11 (2023), 6974–6983. https://doi.org/10.12998/wjcc.v11.i29.6974.

[28] R.S. Tsay, Analysis of Financial Time Series, Wiley, 2005.

[29] W.J. Tsay, W.K. Härdle, A Generalized ARFIMA Process with Markov-Switching Fractional Differencing Parameter, J. Stat. Comput. Simul. 79 (2009), 731–745. https://doi.org/10.1080/00949650801910239.

[30] X. Zhang, T. Zhang, A.A. Young, X. Li, Applications and Comparisons of Four Time Series Models in Epidemiological Surveillance Data, PLoS ONE 9 (2014), e88075. https://doi.org/10.1371/journal.pone.0088075.